Computational Geosciences (2020) 24:1541–1556
https://doi.org/10.1007/s10596-020-09963-4

ORIGINAL PAPER

A deep learning perspective on predicting permeability in porous media from network modeling to direct simulation

Moussa Tembely[1] · **Ali M. AlSumaiti**[1] · **Waleed Alameri**[1]

Received: 19 June 2019 / Accepted: 30 March 2020 / Published online: 20 May 2020

Abstract

Predicting the petrophysical properties of rock samples using micro-CT images has gained significant attention recently. However, an accurate and an efficient numerical tool is still lacking. After investigating three numerical techniques, (i) pore network modeling (PNM), (ii) the finite volume method (FVM), and (iii) the lattice Boltzmann method (LBM), a workflow based on machine learning is established for fast and accurate prediction of permeability directly from 3D micro-CT images. We use more than 1100 samples scanned at high resolution and extract the relevant features from these samples for use in a supervised learning algorithm. The approach takes advantage of the efficient computation provided by PNM and the accuracy of the LBM to quickly and accurately estimate rock permeability. The relevant features derived from PNM and image analysis are fed into a supervised machine learning model and a deep neural network to compute the permeability in an end-to-end regression scheme. Within a supervised learning framework, machine and deep learning algorithms based on linear regression, gradient boosting, and physics-informed convolutional neural networks (CNNs) are applied to predict the petrophysical properties of porous rock from 3D micro-CT images. We have performed the sensitivity analysis on the feature importance, hyperparameters, and different learning algorithms to make a prediction. Values of R^2 scores up to 88% and 91% are achieved using machine learning regression models and the deep learning approach, respectively. Remarkably, a significant gain in computation time—approximately 3 orders of magnitude—is achieved by applied machine learning compared with the LBM. Finally, the study highlights the critical role played by feature engineering in predicting petrophysical properties using deep learning.

Keywords Digital rock physics · Porous media · Finite volume method · Lattice Boltzmann method · Pore network modeling · Tensor flow · Machine learning · Deep learning

1 Introduction

Accurate and fast computation of the properties of subsurface porous media properties is required in many applications, including contaminant cleanup, the oil and gas industry, capturing subsurface CO_2 flow, and gas diffusion layer (GDL) in fuel cells. However, characterizing complex rock such as carbonate remains very challenging due to the intrinsic heterogeneities occurring at all scales of observation and measurement [1]. One of the most important petrophysical properties of reservoir rock is the permeability, which is a function of the complex microstructure of the rock, fluid properties (density, viscosity), and parameters (velocity). Since there is no simple universal correlation for the permeability, an accurate and efficient numerical tool to predict it is highly desirable. The Darcy scale properties can be measured experimentally, which can be time consuming and expensive (particularly for two-phase flow) and allows only a limited set of operating conditions; in that context a data-driven approach can help to generalize and potentially reduce bias in laboratory measurements. Alternatively, a reliable numerical model can be developed to predict the flow properties. The permeability is determined by the rock's type, texture, effective porosity, pore throat size, and pore geometry, in addition to the connectivity and the pore distribution within the network. The importance of rock permeability dictates the fluid flow in a reservoir. To achieve a commercially desirable oil and gas production rate a certain level of permeability is imperative.

✉ Moussa Tembely
moussa.tembely@ku.ac.ae,moussa.tembely@concordia.ca

[1] Department of Petroleum Engineering, Khalifa University, Abu Dhabi, UAE

Pore-scale simulations can be classified into 2 categories: (i) pore-network models [2] and (ii) direct models, which range from finite difference, [3], finite element [4], and finite volume techniques [5, 6] to the lattice Boltzmann method (LBM) [7]. One of the limitations of digital rock physics (DRP) is the computing power required to perform the simulations. Instead of direct simulation, the pore network model is preferred for predicting petrophysical properties due to its simplicity. However, this method, which is based on a simplified network geometry, can hardly provide an accurate estimate. To circumvent the limitations inherent to PNM, we develop a machine learning (ML) algorithm for accurate and fast numerical computation of the permeability. The framework developed can be extended to any properties of multiphase flows in porous media.

Currently, machine learning (deep or not) is one of the most popular scientific research trends within artificial intelligence (AI) and has progressed rapidly in recent years. ML has been used successfully to analyze complex interactions. Complex tasks, such as generating a caption for a given image, have recently been completed using deep learning (DL) [8]. ML has been used to tackle industrial applications ranging from engineering problems to medical diagnostics [8–10]. Nevertheless, in petroleum engineering, most of the applications are concerned with reservoir characterization, estimating petrophysical properties from wells, rock typing, production, and, very recently, drilling optimization [11]. Few studies have been devoted to direct prediction of petrophysical properties using micro-CT images. Although neural networks provide superior predictions for complex problems, there have been only limited efforts to use it with DRP to predict petrophysical properties. However, recently, in [12], an attempt has been made to predict permeability using machine learning; however, the model relies on less reliable PNM approach as output of the machine learning algorithm. In addition, petrophysical feature engineering was neither analyzed nor incorporated. In [13], simple 2D synthetic images without correlation with actual rocks were tested for predicting the permeability using a convolutional neural network (CNN). They showed that a physics-informed CNN is able to predict the permeability to within 10%, in contrast with the Kozeny-Carman equation, which yields relative errors of over 200%. Along the same line in [14, 15], 2D thin section images were used to estimate permeability using CNN by mapping the 2D image from Sandstone core plugs to the measured permeability. Although limited to a representative 2D image of the sample, the approach highlights the applicability and generalization of DL to predict flow properties.

In [16], a CNN is used to predict the porosity, coordination number, and average pore size. However, the more challenging task of predicting the permeability is not considered. Finally, the recent work in [17] on segmenting synthetic rock images using machine learning is noteworthy; the results showed a good classification rate compared with traditional segmentation techniques. However, the study did not address the prediction of petrophysical properties. Despite the widespread application of PNM in DRP, it suffers from some inherent limitations. One the major issue with PNM is the simplification of the pore-space geometry and fluid flow dynamics. To overcome these limitations, it is essential to conduct simulations that solve the appropriate governing equations directly in a representation of the pore space. However, due to high computational cost of direct methods such as the LBM, it is difficult to accommodate all the relevant flow physics and details of the pore geometry. In most approaches, the premise is that the permeability derived through PNM represents the actual permeability of the sample [12]. In fact, as we show in the present study, there is a significant discrepancy between the more accurate permeability computed using the LBM and the value from PNM. Machine learning (deep or not) could be an attractive alternative for predicting petrophysical properties.

In [18], an interesting approach is developed to accurately predict the pore network conductances based on pore shape parameters using machine learning. The model is trained on 2D images extracted from 3D micro-CT of 2 samples—carbonate and sandstone. The prediction of the conductance is found to be over 90%. However, the estimation of the permeability from 3D micro-CT is not addressed; notwithstanding, this approach is expected to significantly improve PNM pretrophysical prediction compared with current approaches relying on the geometrical simplification of the pore space. A pore network combined with LBM is proposed in [19]. Due to its accuracy, the LBM is used to compute the permeability of the different pore throats from the pore network, which is more accurate than simply using Hagen-Poiseuille relation on cylindrical pore throat shape. Overall, the LBM computational cost is reduced by using image-based features to estimate LBM throat permeabilities using machine learning.

In [20, 21], a distributed parallel GPU implementation of LBM based on the multiple-relaxation-time (MRT) model is proposed and tested; this approach enables speeding up the computation up to 10-fold compared with classical implementation of LBM. The present work aims to reduce even further the computational cost of the permeability with fewer resources.

In addition, an application to two-phase flow is performed in [22], highlighting the capability of the approach to handle complex problems involving transient two-phase flow. In [23], an interesting application of generative adversarial neural networks (GAN) to generate porous media using previous micro-CT images of rocks. Interestingly, the synthetic images generated retrieve both

the statistical and petrophysical properties such as the permeability of the rock.

In the present paper, using 3D micro-CT images, a comparative study of 3 numerical techniques for simulating flow properties is performed in the context of digital rock physics (DRP). A pore network is generated from the segmented images using a maximal ball algorithm; then, the simplified network is used as input of the PNM for computing both the permeability and the formation factor. In addition, using the same segmented images, a more complex geometry is constructed and meshed for a FVM simulation that computes the permeability. Finally, a *voxel-based* version of the lattice Boltzmann method (LBM) is employed to predict the permeability directly from the binary images. The computationally intensive nature of the simulations is strongly related to the complexity of the pore structure generated, and the accuracy is affected by simplifying the geometry. In addition to discussions on the advantages and limitations of the 3 numerical different techniques, a machine (deep or not) learning framework is detailed for a fast and accurate estimation of the permeability from 3D micro-CT images.

The paper is organized as follows: in Section 2, numerical techniques for flow property simulation are detailed; and in Section 3, data analysis and a workflow based on machine learning are presented in order to make permeability prediction using supervised learning (subsection 3.1) and deep learning based on multilayer perceptron (MLP) and CNN (subsection 3.2); and finally conclusions are drawn in Section 4.

2 Numerical techniques

Our goal was to develop a workflow capable of predicting petrophysical properties from micro-CT images of rock. In the present case, we investigated machine learning algorithms combined with numerical techniques to simulate fluid flow within a 3D digital rock. We applied two widely used approaches, network modeling and direct simulation, through three numerical techniques: PNM, FVM, and LBM. Void structures in network modeling are approximated as pores connected by throats, while LBM uses the voxel grid directly; FVM operates on a simplified and meshed voxel grid. The complexity of the network dictates the computational cost. Since network modeling is less rigorous than direct simulation models, the approach is computationally cost effective at the expense of the simulation accuracy. The workflow to be developed will help to establish a fast and accurate prediction of rock permeability. The following sections present the methodology, and governing equations of the three numerical techniques to compute the permeability from digital rock images will be detailed.

2.1 Pore network modeling

PNM simulation entails a network of pores and throats that topologically correspond to the pore structure of the rock, which is extracted directly from the micro-CT images. The flow rates, (Q_{ij}), within the throats between each pair of adjacent pores (i, j) of the network, are given by:

$$Q_{ij} = -\frac{r_{ij}^4}{8\mu l_{ij}}(p_j - p_i), \tag{1}$$

where p_i and p_j are the pressures at nodes i and j, l_{ij} corresponds to pore throat length, and r_{ij} represents the pore throat radius; μ is the viscosity. Considering mass conservation at internal pores, we have:

$$\sum_i Q_{ij} = 0 \tag{2}$$

which leads to a system of equations that enables the computation of pressure in each pore.

After solving for the pressure and the flow rate, the permeability can be computed following Darcy's law as follows:

$$K = \frac{\mu L Q}{A_o \Delta P} \tag{3}$$

where A_o is the outlet surface area of the sample and Q is the overall flow rate computed by integration from the outlet of the sample, while ΔP is the pressure gradient imposed. In addition to the permeability, the formation resistivity factor was computed. It quantifies the impact of pore space on the resistance of the sample, and is defined as follows:

$$F = \frac{R_o}{R_w} \tag{4}$$

where R_o is the resistivity of fully water-saturated rock, and R_w is the saturating water resistivity. The formation factor accounts for both the porosity and the tortuosity of the sample. The quantitative predictive potential of PNM was investigated on networks extracted using the maximal ball algorithm [2].

2.2 The finite volume method

The continuity and momentum equations to be numerically solved by the finite volume method (FVM) are expressed as follows:

$$\nabla.\mathbf{V} = 0 \tag{5}$$

$$\rho\nabla.(\mathbf{VV}) = -\nabla p + \rho\mathbf{g} + \nabla.(\nabla\mu\mathbf{V}) \tag{6}$$

where $\mathbf{V}$ is the fluid velocity vector and $\mathbf{g}$ denotes gravity, while the fluid is assumed incompressible of density ρ and viscosity μ. The pore space is meshed based on the micro-CT images. After solving the fluid flow equations,

mass, and momentum conservation, the permeability was computed using the relation given above in Eq. (3).

2.3 The lattice Boltzmann method

This technique of a single-time relaxation scheme based on BGK collision operator was used to predict the permeability. The fluid taken as a set of particles satisfies the following evolution equation for the distribution function $f(x,t)$:

$$f(x+e_i,t+1) = \frac{1}{\tau}(f(x,t) - f_{eq}(x,t)) = \Omega(x,F,\tau,t) \tag{7}$$

where e_i is the particle velocity in the i^{th} direction, τ is the relaxation time, Ω is a collision operator, and F is an external force term such as gravity in the present case. Finally, based directly on the binary images, the permeability is derived as in subsection 2.1 using Darcy's law Eq. (3).

2.4 Implementation of fluid flow and machine learning codes

The pore network used the maximal ball algorithm for network extraction. The code details are provided in [2]. FVM was based on OpenFOAM/C++ and details of the code can be found in [6]. The LBM simulation used the parallel lattice Boltzmann solver (Palabos) code, written in C++, to perform the simulation at the pore scale using the segmented images as input. Supervised learning techniques were based on (i) machine learning through the Scikit-learn library and (ii) deep learning algorithms using TensorFlow combined with the Keras framework. All the codes use open-source libraries implemented in Python and C++. While PNM was run on a single node, FVM and LBM were run in parallel using domain decomposition techniques on 2 nodes of 16 CPU cores with 64-GB RAM per node. Regarding the deep learning model using CNN, the training was performed through an HPC on 2 GPU nodes having 4 NVidia K80 GPU cards with 128-GB RAM per node. Moreover, the LBM input was $152 \times 152 \times 175$ voxels while the meshed geometry for FVM consisted of 32,345,600 cells. Further details on the implementation can be found in [6, 24].

2.5 Simulation of fluid flow properties

Regarding the application of the three techniques, for the simulation, we considered high-resolution rock samples from the literature and our own complex carbonate samples. The dataset consisted of 400 segmented samples of size $152 \times 152 \times 175$ voxels at 2 μm resolution, and another set of 759 images of size $100 \times 100 \times 160$ voxels extracted from the micro-plug scanned at 0.48 μm (Fig. 1). While

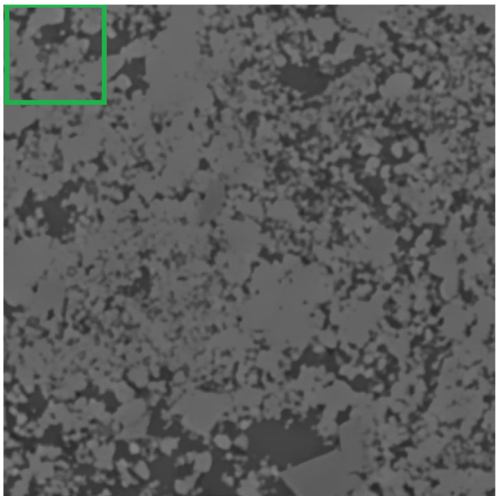

Fig. 1 Micro-CT image of a rock sample scanned at high resolution. The extracted sub-sample is highlighted by the square box.

the first data provided by IFPEN was already segmented, an automatic Otsu's algorithm was used to segment our own (second) dataset for simulation purposes.

First, we focused on the first dataset from the literature to establish our workflow for predicting petrophysical properties. To apply the PNM technique from the segmented images, the network was extracted using the maximal ball algorithm [2]. Figure 2 shows the statistics of the pore structure of the three samples. We provide below the pore network structure in terms of pore diameter, throat diameter, and length distribution, exhibiting complex structures over a wide range of length scales.

The numerical simulation was performed on the three samples using the three numerical techniques: PNM, FVM, and LBM. For illustrative purpose, Fig. 3 shows the approaches of the PNM and FVM to simulate the permeability from a rock scanned at high resolution. It is worth noting that in the present case of simulating on 3D micro-CT images of rocks, LBM was performed directly on the raw segmented images while FVM needed the pore space to be meshed. This is very challenging and involves the simplification of pore geometry. As a result, FVM can be considered less accurate than LBM in the context of digital rock simulation [20].

This section presents an assessment of the three numerical techniques. The results of the simulation computing the permeability are summarized in Table 1. Both FVM and LBM were more accurate than PNM (Fig. 4). However, the computation time of PNM was two and three orders of magnitude faster than FVM and LBM, respectively (Table 2).

It is worth noting that we just accounted only for the execution time to run the case. The mesh and network generation required for PNM and FVM were not considered since different test cases can be run after the network or

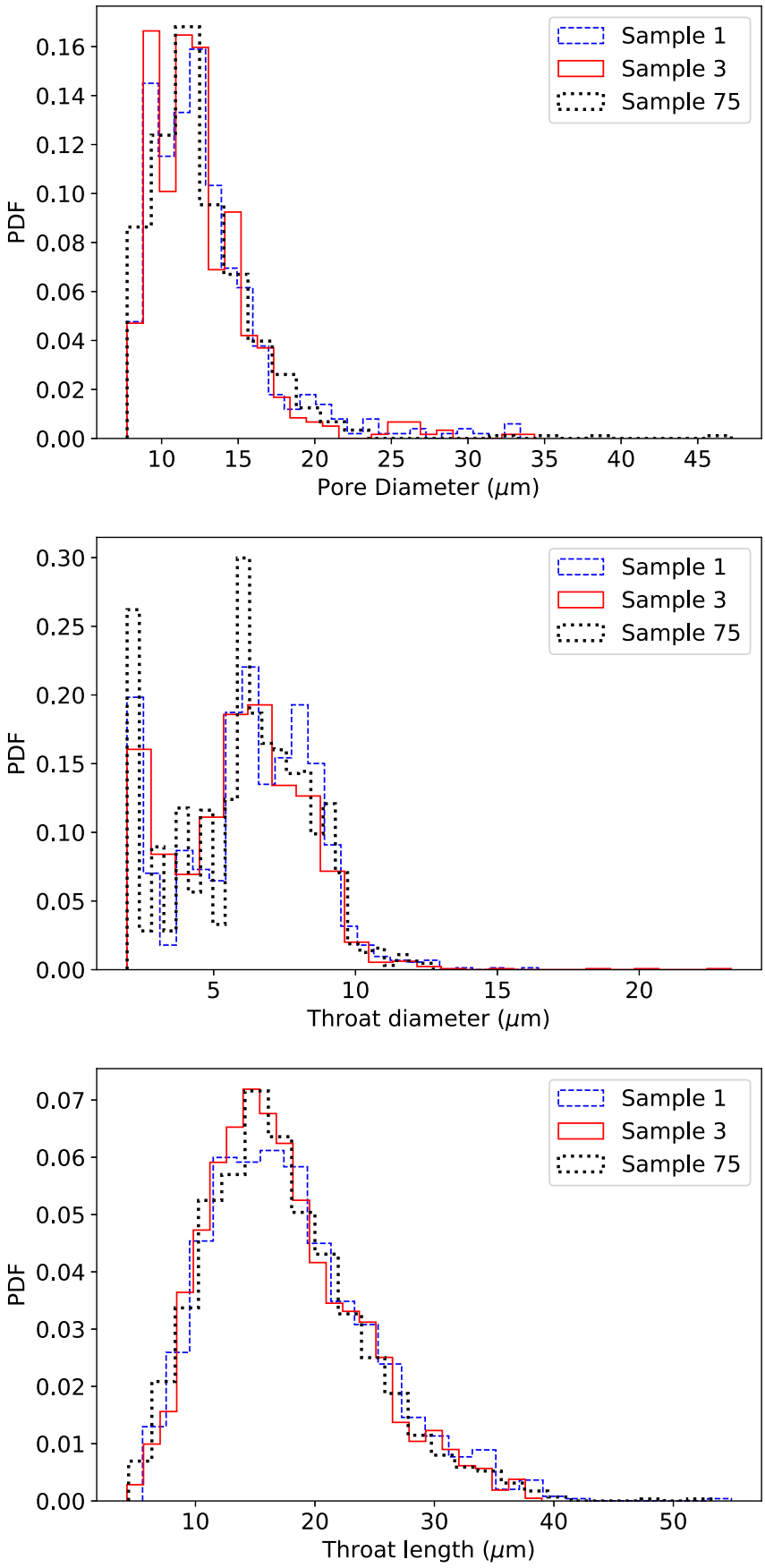

Fig. 2 Statistics of the pore network extracted from three samples. The probability distribution function (PDF) is expressed in terms of pore diameter, throat diameter, and throat length, respectively.

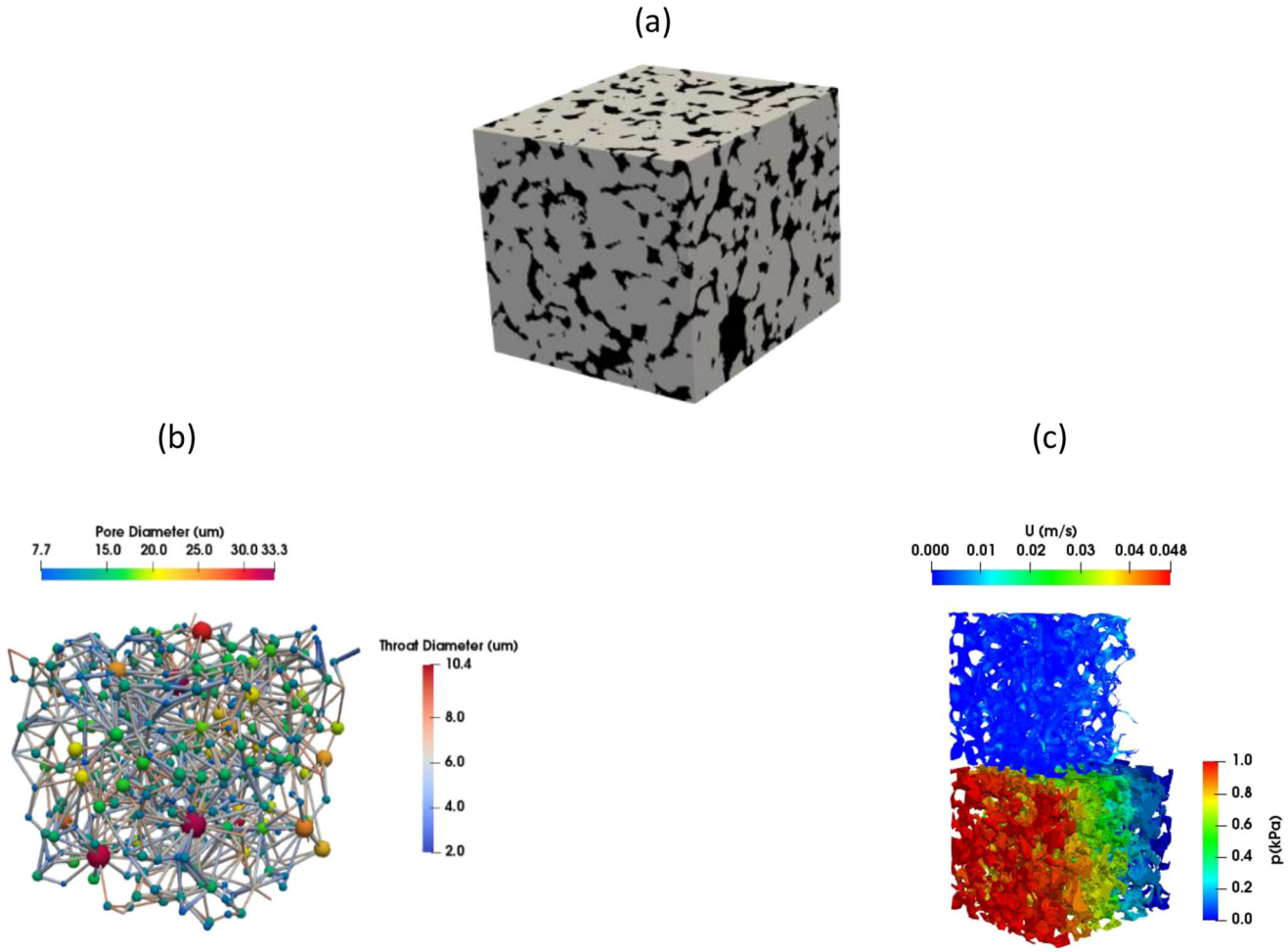

Fig. 3 Approach and geometry used by the three numerical techniques (**a** LBM, **b** PNM, and **c** FVM) for simulating sample 1 scanned at high resolution.

mesh generation. The discrepancy observed for the PNM techniques is in line with findings elsewhere [2]. The simulation time of LBM is an order of magnitude longer than the FVM. However, PNM runs instantly once the network is extracted, which is a relatively fast operation by using the modified maximal ball algorithm. A major advantage of PNM is that the compromise made on the details of geometrical and topological representation allows PNM to simulate much larger domains and simulate them more efficiently. While PNM can suffer from a lack of accuracy, however, it can easily be used to provide an insight into the multiphase flow properties within porous media. Due to its simplicity, PNM is traditionally used to compute both single and multiphase petrophysical properties of rocks within the DRP framework.

Table 1 Permeability (in mD) for three samples based on the three numerical techniques. For convenience, the relative errors with respect to LBM results are provided in parentheses

Sample no.	PNM (error)	FVM (error)	LBM
Sample 1	112.42 (10.80%)	113.04 (10.30%)	126.03
Sample 3	111.59 (9.29%)	93.72 (8.20%)	102.10
Sample 75	204.11 (29.11%)	112.09 (29.09%)	158.09

Finally, to assess the model's predictive capability, we used an R^2 score or coefficient of determination to measure how well samples are likely to be predicted by the model. It is defined as follows:

$$R^2 \text{ score} = 1 - \frac{\sum_{i=1}^{Nsple} y_i - \tilde{y}_i}{\sum_{i=1}^{Nsple} y_i - \bar{y}_i} \tag{8}$$

where y_i and $\tilde{y}$ represent the target and predicted values, respectively, while $\bar{y} = \sum_{i=1}^{Nsple} y_i / Nsple$, where $Nsple$ is the number of samples considered. It is worth noting that the best possible score is 1.0; however, it can be negative if the model is arbitrarily worse.

We show below in Fig. 5 an estimation of the accuracy of PNM with respect to LBM; R^2 scores of about

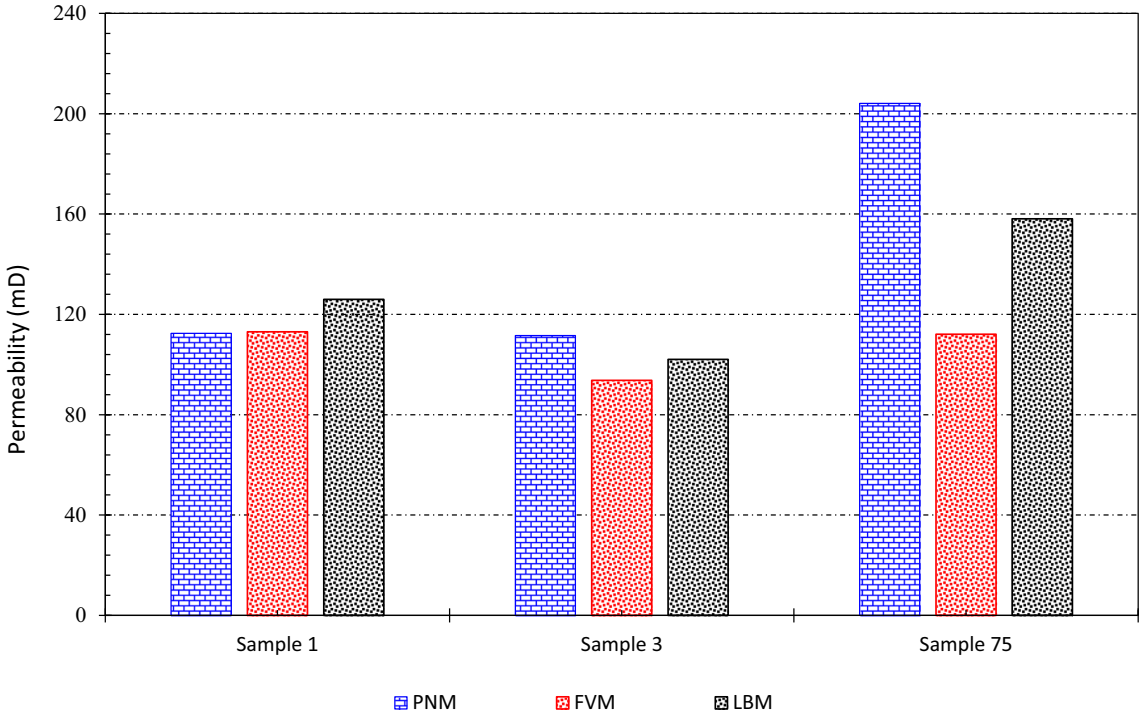

Fig. 4 The results of the permeability prediction on the three samples

Table 2 CPU time from the 3 numerical techniques

Techniques	PNM	FVM	LBM
CPU time (s) 2 × 8 core 16GB	1	121	2400

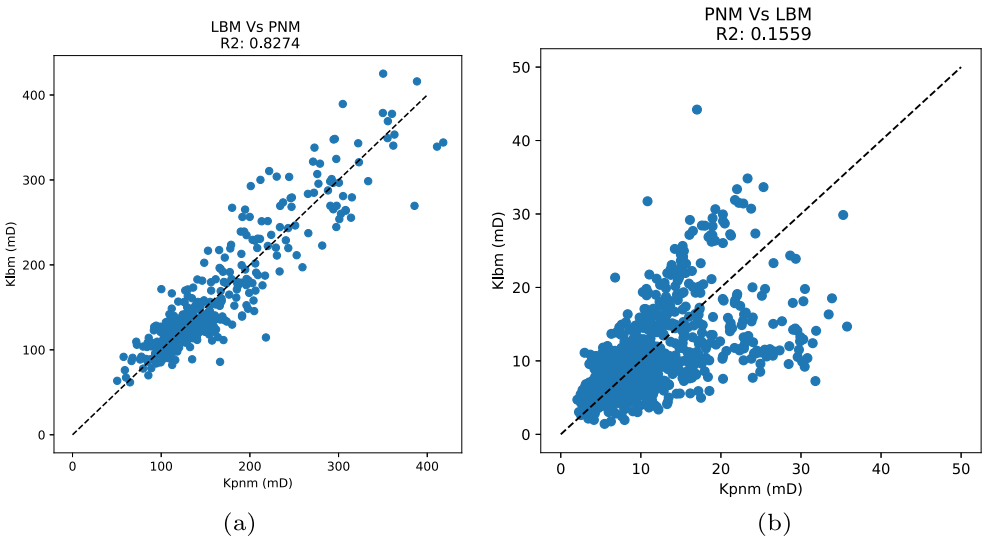

Fig. 5 R^2 score derived from the cross-plot between LBM and PNM permeabilities of two datasets: **a** from the literature and **b** from our own complex carbonate samples

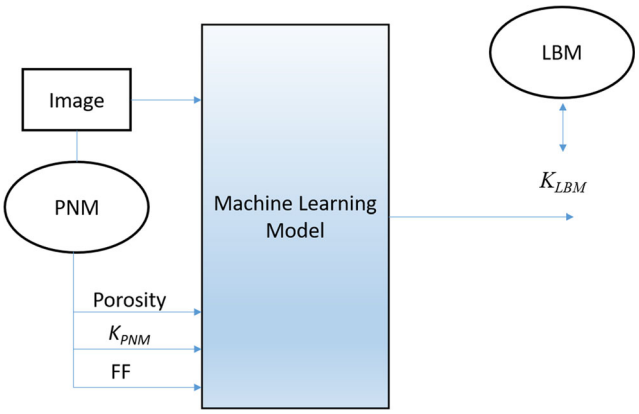

Fig. 6 Schematic of the machine learning framework for a fast and accurate prediction of the permeability

82% and 16% were found for the 2 datasets considered. This highlights the poor predictive capability of PNM against LBM. The goal of the present work is to improve the accuracy of network modeling permeability through machine and deep learning.

3 Data generation and analysis for machine learning

Due to the efficient computational cost, we used the PNM technique to extract the following features from our dataset: porosity, permeability, and formation factor, to use machine for learning. While the porosity is estimated directly from the segmented image, the permeability and the formation

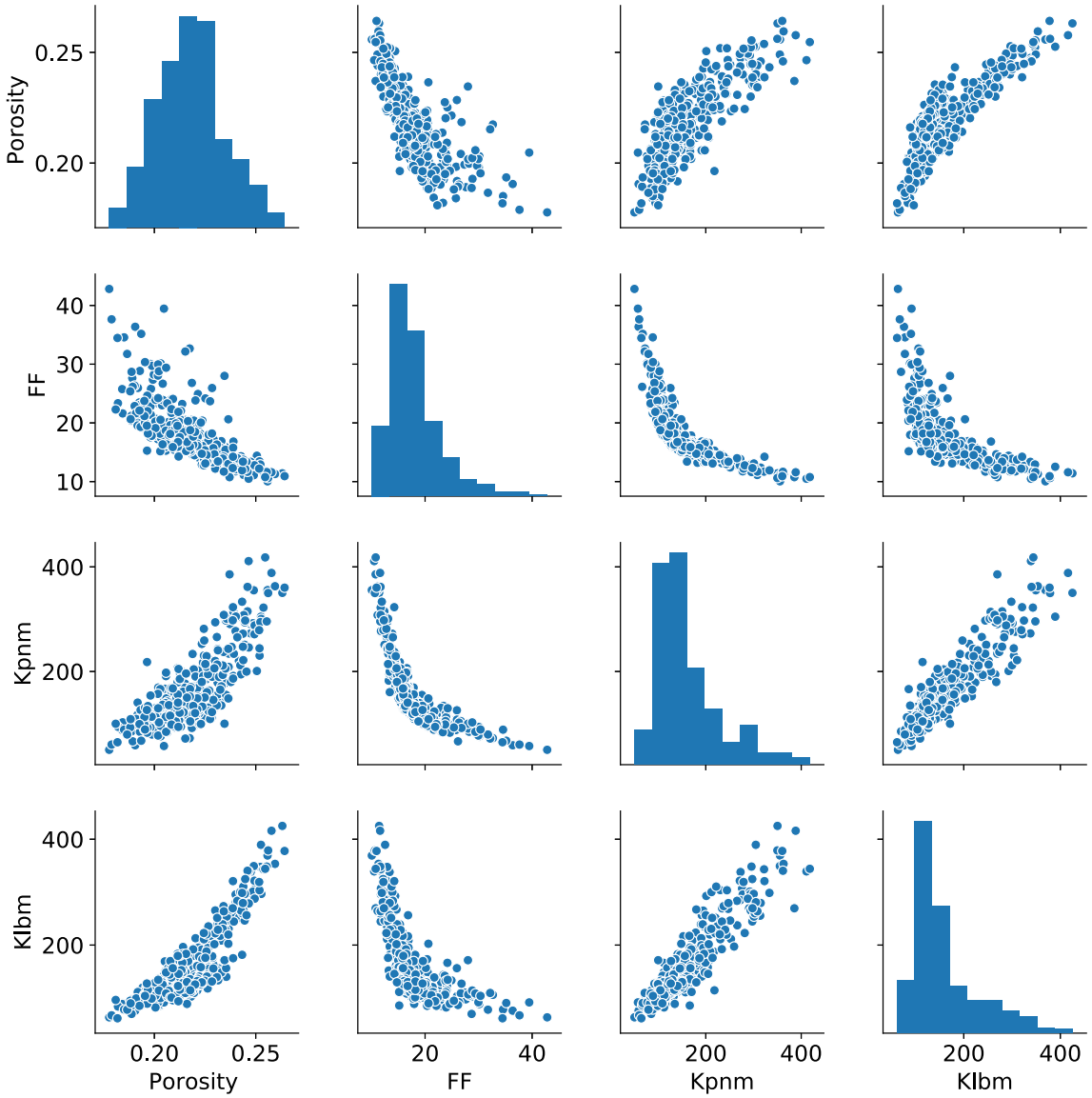

Fig. 7 Cross-plots of the generated features for machine learning purposes

Table 3 Statistics on the features extracted from the 400 samples

Properties	Porosity	FF	K_{pnm}	K_{lbm}
Count	400	400	400	400
Mean	0.22	18.00	159.71	160.63
std	0.017	4.93	68.02	69.79
min	0.18	10.05	50.36	61.70
25%	0.21	15.10	113.22	114.55
50%	0.22	16.86	139.20	135.58
75%	0.23	20.04	187.29	181.92
max	0.26	42.82	418.05	425.13

factor are determined using pore network modeling. Like permeability, the formation factor is a function of the rock texture, structure, and connectivity. Besides the features derived by PNM, direct simulations with LBM were used to compute the permeability of all the 400 (simple) and 759 (complex) samples. ML was expected to reduce significantly the computational time compared with direct simulations with comparable accuracy.

We show in Fig. 6 the structure of the machine learning algorithm from the input image and the features extracted from PNM to the predicted permeability (K_{LBM}).

We present below in Fig. 7 an overview of the dataset from the literature by presenting the cross-plot of the porosity, formation factor, and PNM permeability, compared with the more accurate LBM permeability. The statistics of the dataset are summarized in the Table 3. The results highlight the fact that the PNM cannot be predictive of the actual permeability (by LBM) of the sample. While PNM is widely used for simulating petrophysical properties, these results suggest a simplified representation should be corrected if it is to be used as a reliable tool for prediction.

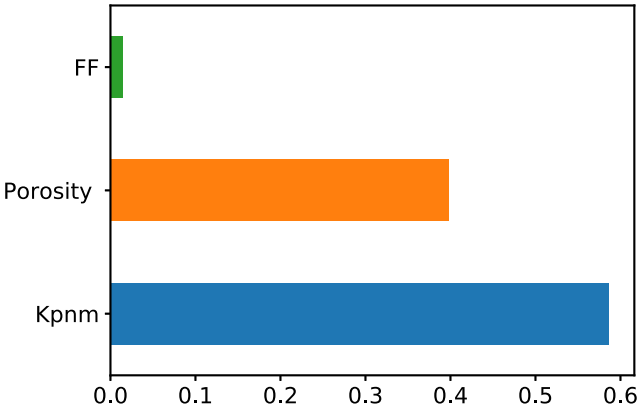

Fig. 9 The different features and their relative importance used for machine learning.

In the following, we used both (i) a supervised machine learning technique and (ii) a deep neural network to infer on rock permeability. We first trained the model using both the input (values for the selected features) and output data (permeability values). Then, we used the model to predict the test data.

3.1 Supervised regression models

We used regression problem aiming to predict a real-valued output. We used both linear and gradient boost techniques to improve the two models. Feature cross techniques were assessed as well. From our dataset, 70% of the data were used as the training set while 30% of the data were used as the test set. We first fit the model on the training data and then predicted using the holdout test samples. Since the train/test split method may not be fully random, to validate the model, we used k-fold cross-validation in conjunction with machine learning algorithms. In k-fold

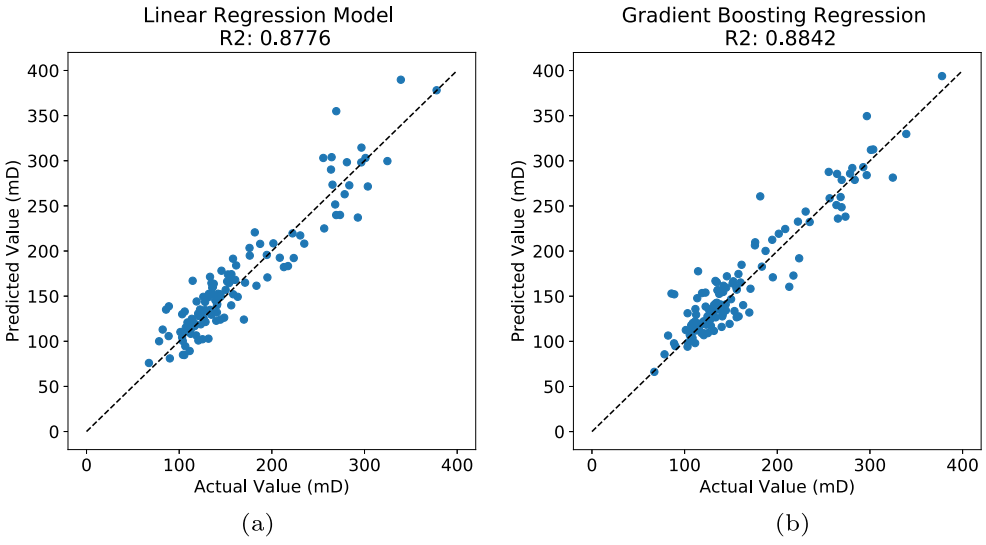

Fig. 8 The prediction of permeability using **a** linear and **b** gradient boost regression algorithms, respectively

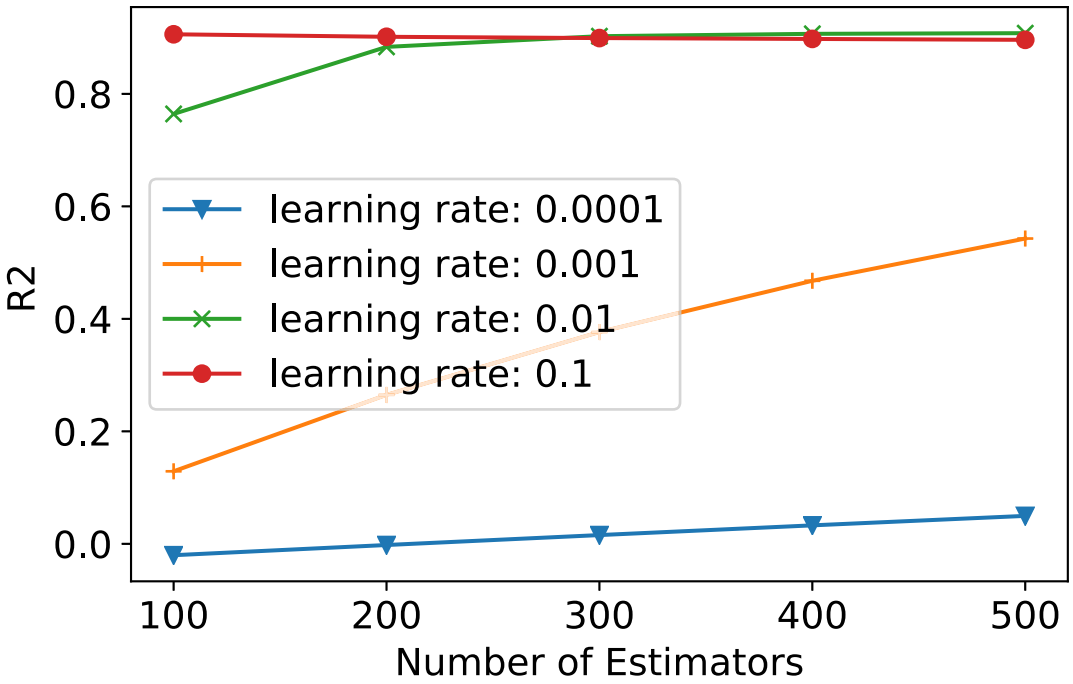

Fig. 10 Sensitivity test of the hyperparameters used for machine learning

cross-validation, we split our data into k different subsets (or folds). We used $k-1$ subsets to train our data and left the last subset (or the last fold) as test data. In our case, we took $k=5$, and then averaged the model against each of the folds. Figure 8 shows the result of prediction using a linear regression and gradient boost algorithms on the test data. There was a slight improvement using the gradient boost method compared with the linear regression model.

The overall score of the gradient boost algorithm using k-fold technique resulted in 88.42% with a standard deviation of 3.96%. In addition, we evaluated feature importance on the predictive capability of the machine learning algorithm, and we found (in Fig. 9) that the dominant feature, not surprisingly, was the PNM permeability (58.6%) followed by the porosity (40%) and the formation factor (1.4%).

It is worth noting that the hyperparameters were optimized using a technique that combined grid search and k-fold cross-validation. For the gradient boost algorithm, this led to the following hyperparameter variation for the learning rate and number of estimators (Fig. 10); we chose a learning rate of 0.1 and number of estimator of 100 for the model prediction.

To extend the previous ML models, we added the feature cross technique to the linear regression algorithm and gradient boost algorithm. We found that the best feature cross corresponded to polynomial combinations of the

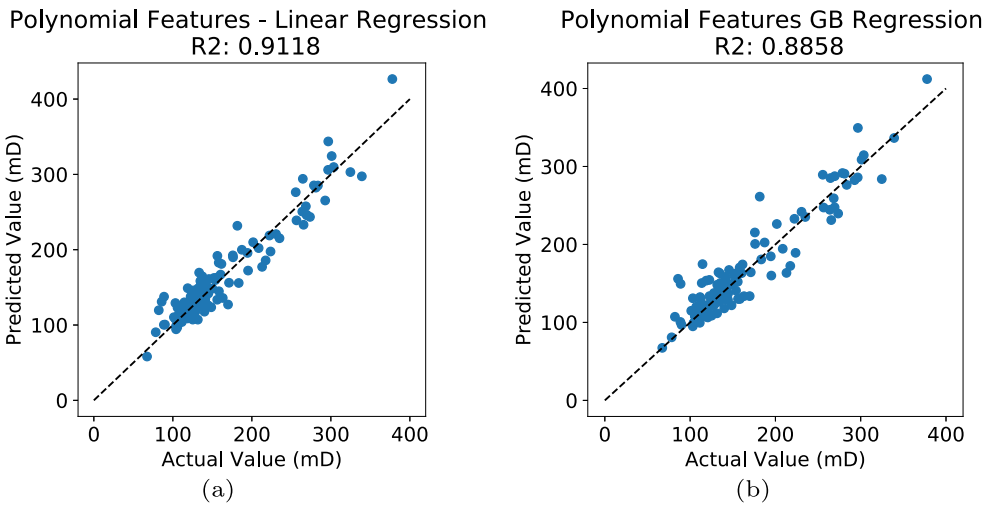

Fig. 11 Feature crosses using polynomial combinations of the features with degree less than or equal to 2 for both **a** linear algorithm and **b** gradient boost algorithm

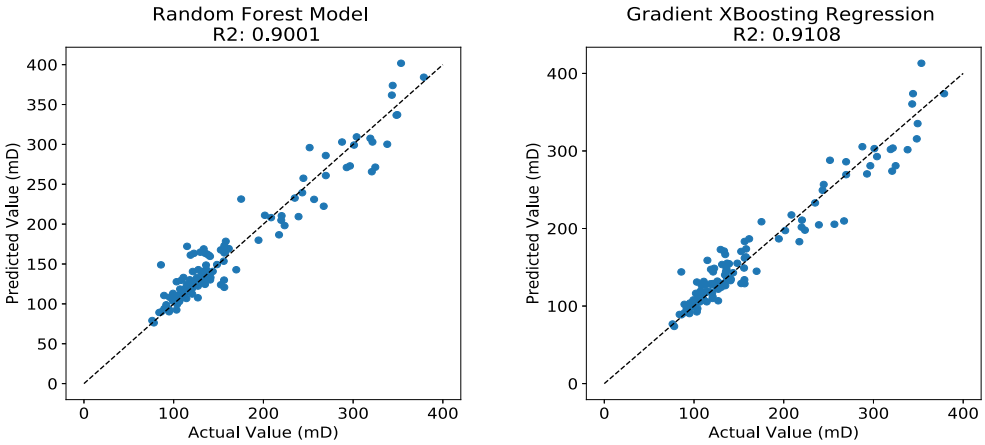

(a) (b)

Fig. 12 The prediction of the permeability using **a** random forest and **b** improved gradient boost regression algorithms, respectively.

features with a degree less than or equal to 2. Interestingly, the linear regression performed better than the gradient boost by incorporating feature cross in the models (Fig. 11), unlike in the previous case in Fig. 8 without feature cross.

To further our analysis, we tested the random forest (RF) algorithm and extreme (or improved) gradient boosting (XGB) algorithm (Fig. 12). These two models helped improve the accuracy of the prediction compared with the previous algorithms.

In addition, we investigated the model's sensitivity to the different features in Fig. 13. We added features extracted from the PNM model, such as the ratio of the median throat length to the radius and the average connection number. As the FF feature seems less important, we tested the model with and without it. The result is shown in Fig. 13, which compares the case of two features (porosity and K_{pnm}) to five features: porosity, K_{pnm}, the ratio of the median throat length to the radius ratio, and the average connection number. This yielded a marginal improvement of the model's performance in considering five features instead of two.

3.2 Deep neural network model

To complement the previous analysis in machine learning, we used deep learning based on multilayer perceptron (MLP) architecture to investigate the permeability from the features derived previously. To make the model non-linear, an activation function was used such that the relation between input ($\mathbf{x}$) and output ($\mathbf{y}$) of one layer can be represented as:

$$\mathbf{y} = \sigma[w\mathbf{x} + b] \tag{9}$$

The reLU rectified linear unit activation function was used in this study. A neural network with one layer of intermediate variables between input and output (one hidden

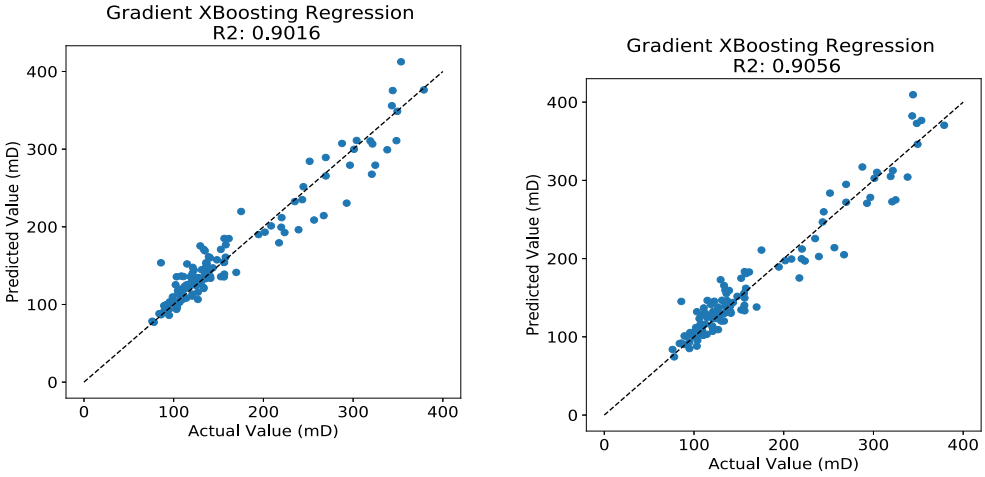

(a) (b)

Fig. 13 The prediction of permeability using an improved gradient boosting regression algorithm on **a** two features and **b** five features, respectively

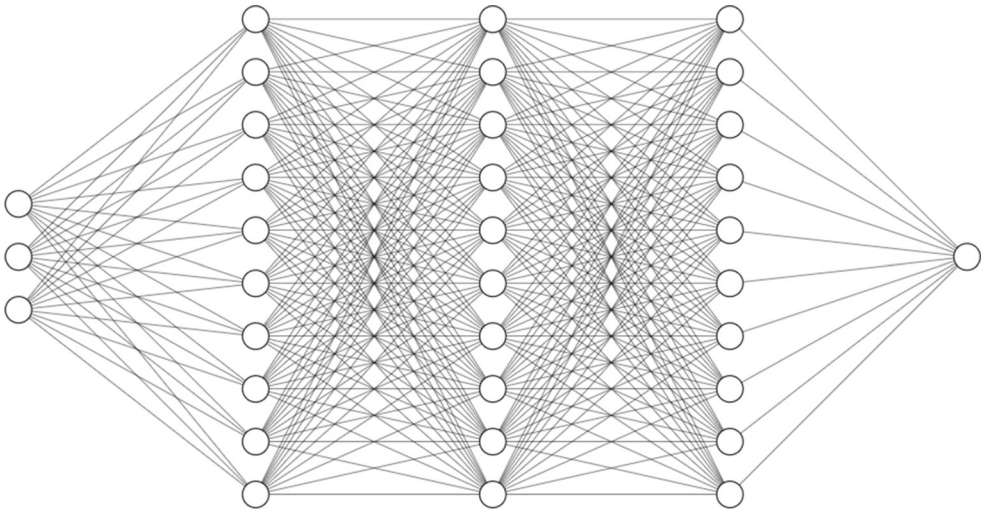

Fig. 14 Architecture of the base model used for the deep neural network

layer) may be represented by Eq. (9). A deep neural network (DNN) is defined as sequential layers that data flow through. It consists of connected nodes of multiple layers. The architecture of the first network tested, with 3 hidden layers of 10 nodes, is shown below in Fig. 14. We used a densely connected feed-forward neural network. In other words, there were no loops in the connections between the nodes, and a node in each layer was connected to all the nodes in the next layer.

The result of the prediction by DNN using the base model is shown in Fig. 15, which improves the performance of the previous ML algorithms.

We ensured that the DNN was not overfit by tracking the loss function in addition to the early stopping procedure. Figure 16 shows the variation of the training and validation loss in terms of the number of epochs. This indicates that our model was not overfitting.

We then optimized the base model architecture using the TensorBoard toolkit integrated into TensorFlow. In addition, we tested the deep neural network (DNN) with the feature cross technique. We found an optimized DNN consisting of 4 layers of 64 nodes (Fig. 17a). However, there was no noticeable performance improvement with feature cross (Fig. 17b). Overall, the performance of the DNN model was improved, although only slightly compared with the base model and only marginally with respect to the tree-based machine learning models. The comparable performance between deep learning and machine algorithm could be related to the fact that the size of the dataset was not so large as to show a significant gain in performance provided by deep learning approaches.

Finally, we applied DNN to the second dataset of a complex carbonate, which yielded the following result on the prediction of permeability (Fig. 18). There was a significant improvement from the DNN approach compared

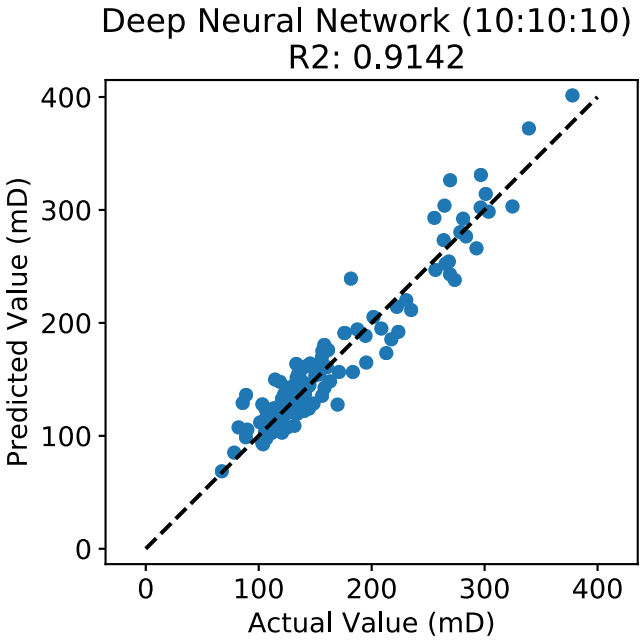

Fig. 15 Base model used for the deep neural network

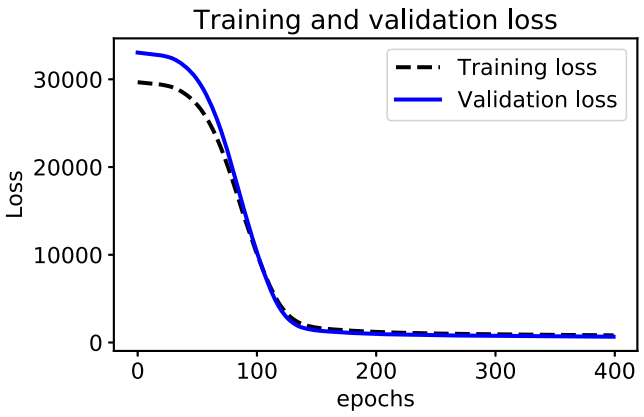

Fig. 16 Loss function in terms of the number of epochs

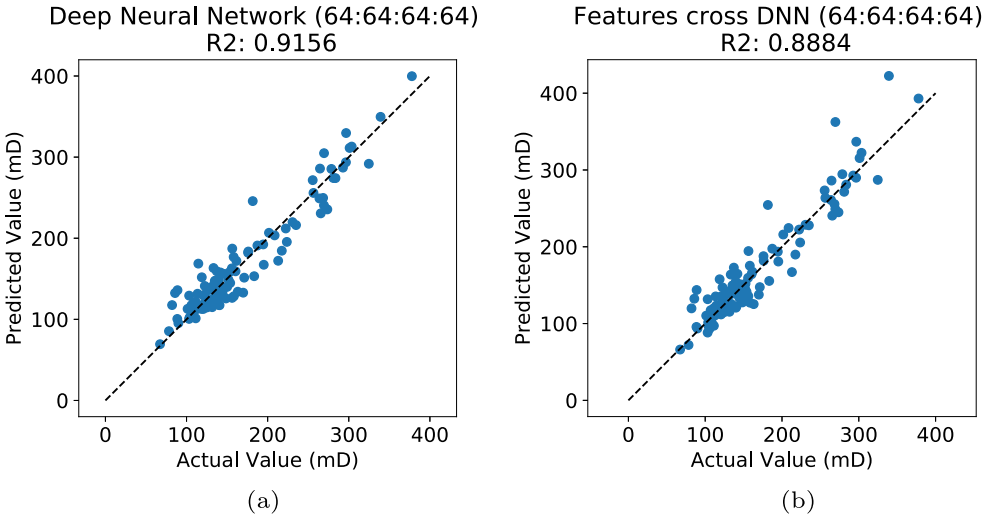

Fig. 17 Prediction by DNN after optimization of the model hyperparameters

with relying on PNM to compute the permeability (Fig. 5b). Furthermore, once the network was trained, the prediction of permeability could be computed in less than a second compared with the resource-intensive LBM simulation of three orders of magnitude slower.

Finally, we implemented a convolution neural network (CNN) approach in which the model used only the raw segmented images. The CNN architecture, consisting of convolution, pooling, and connected dense layers, is given in Fig. 19. The CNN tested consisted of two convolutional layers, each followed by a pooling layer, then by fully-connected layers (Table 4). We tested this model extensively by investigating different architectures. We found that the CNN model alone could not predict at more than 85%.

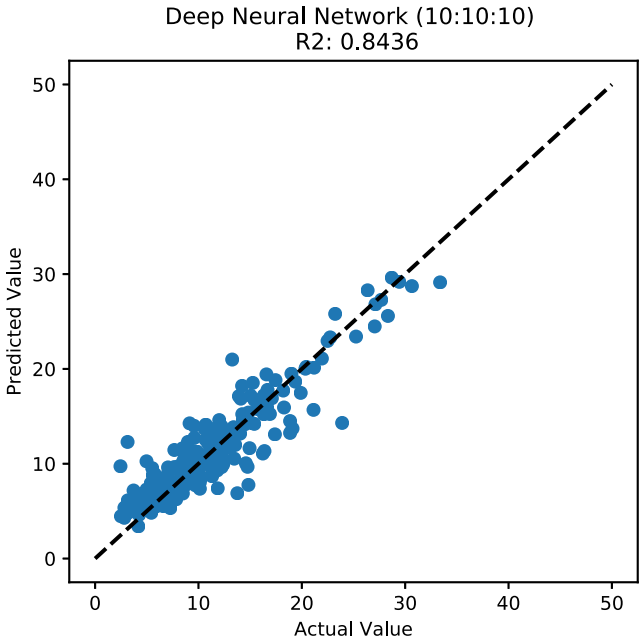

Fig. 18 DNN applied to a complex carbonate dataset

To improve the performance of CNN, we extended it to include some features such as the porosity and the formation factor. The result of the prediction is shown in Fig. 20. Although this physics-informed model is more elaborated, there was no significant improvement in performance compared with DNN. However, differences may appear for larger datasets.

Finally, we provided the performance of the different algorithms in terms of R^2 score tested (Fig. 21). All the models—except the support vector machine (SVR)—performed better than the permeability computed by PNM. Overall, these results highlight the capability of ML and DL to infer pretrophysical properties accurately.

4 Conclusion

We established a machine learning workflow to predict the permeability of porous media quickly and accurately. We first performed a comparative study of three numerical techniques—PNM, FVM, and LBM—to compute the flow properties of rock samples scanned at high resolution. Unlike the widely used technique of PNM, LBM is very accurate but quite resource intensive. To take advantage of the efficient computation provided by PNM and the accuracy of LBM, machine learning algorithms were developed to infer the permeability of a rock scanned at high resolution. Different machine learning algorithms (deep or not) were tested on a dataset containing more than 1000 micro-CT 3D images. The relevant features, such as the porosity, the formation factor, and the permeability according to PNM, along with the 3D images, were fed into both a supervised machine learning model and a deep neural network to compute the permeability. It was found that the DNN performed slightly better than gradient boosting and linear regression with feature crosses. The results provide a

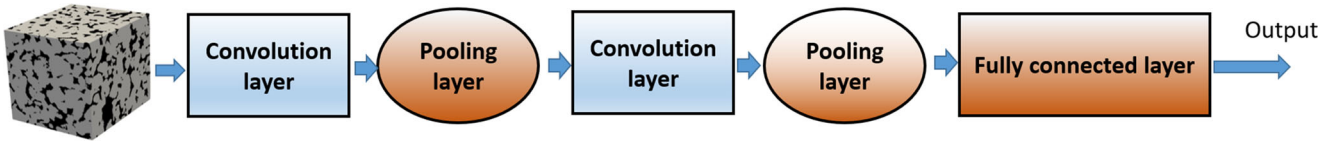

Fig. 19 Schematic of the CNN network for the prediction of permeability

Table 4 The architecture of CNN used.

Operations	parameters	Numbers of layers
3D convolution	Kernel size=(5,5,5) Stride=(1,1) Filters= 1, 1 Activation= ReLU	2
Max Pooling 3D	Kernel size=(4,4,4) Stride=(1,1) Filters= 2 2	
Dense layers	Activation= ReLU Neurones=[8],[8,16], [8,32,64,128]	1, 2, 4

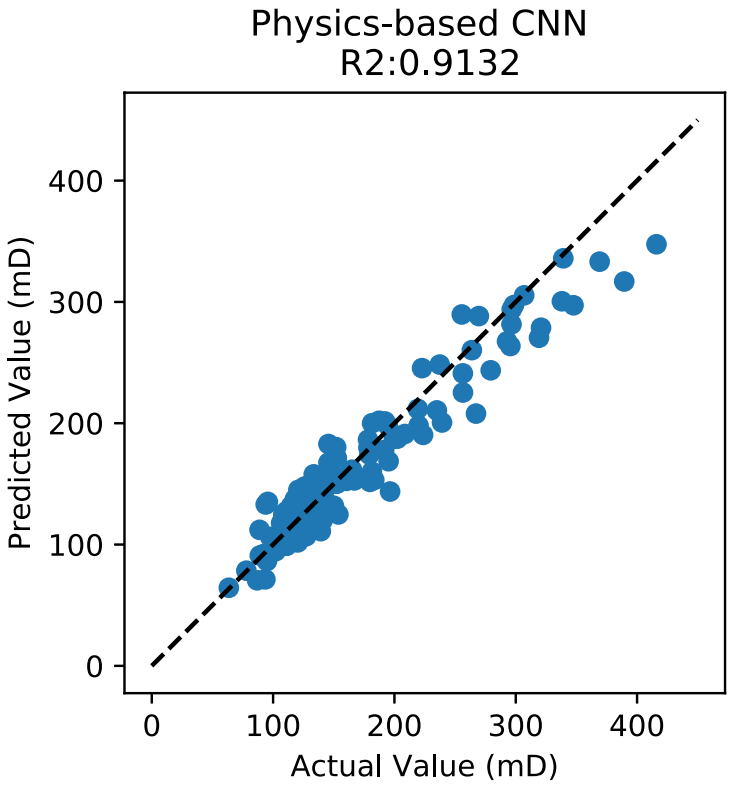

Fig. 20 Physics-based CNN prediction of the permeability

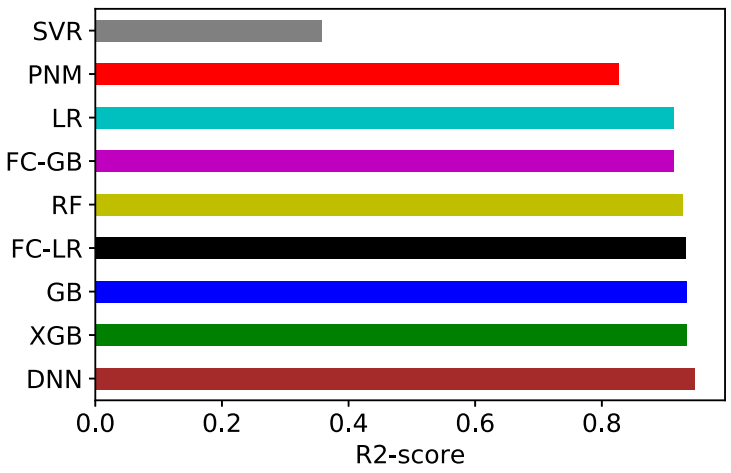

Fig. 21 Summary representation in terms of R^2 score of the different shallow and deep learning algorithms tested

workflow for predicting the petrophysical properties of rock samples based on micro-CT images. Finally, with an accuracy close to 92% and a short prediction time, deep learning was found to be an attractive complement to both traditional PNM and LBM. Therefore, simulations that could take days would need only a few seconds when a trained network is used. For perspective, while the predictions made by convolution neural networks (CNNs) based solely on raw images were not satisfactory in the present study, future developments may help limit the feature engineering required to predict petrophysical properties.

Funding information The authors received financial support from ADNOC and Khalifa University supercomputing resources (HPCC) made available for conducting the research reported in this paper.

Compliance with ethical standards

Conflict of interest The authors declare that they have no conflict of interest.

References

1. Andrä, H., Combaret, N., Dvorkin, J., Glatt, E., Han, J., Kabel, M., Keehm, Y., Krzikalla, F., Lee, M., Madonna, C., Marsh, M., Mukerji, T., Saenger, E.H., Sain, R., Saxena, N., Ricker, S., Wiegmann, A., Zhan, X.: Digital rock physics benchmarks-Part I: Imaging and segmentation. Computers and Geosciences **50**, 25–32 (2013). https://doi.org/10.1016/j.cageo.2012.09.005
2. Dong, H., Blunt, M.J.: Pore-network extraction from micro-computerized-tomography images. Physical Review E - Statistical, Nonlinear, and Soft Matter Physics **80**(3), 1–11 (2009). https://doi.org/10.1103/PhysRevE.80.036307
3. Mostaghimi, P., Blunt, M.J., Bijeljic, B.: Computations of Absolute Permeability on Micro-CT Images. Mathematical Geosciences **45**(1), 103–125 (2013). https://doi.org/10.1007/s11004-012-9431-4
4. Andrä, H., Combaret, N., Dvorkin, J., Glatt, E., Han, J., Kabel, M., Keehm, Y., Krzikalla, F., Lee, M., Madonna, C., Marsh, M., Mukerji, T., Saenger, E.H., Sain, R., Saxena, N., Ricker, S., Wiegmann, A., Zhan, X.: Digital rock physics benchmarks-part II: Computing effective properties. Computers and Geosciences **50**, 33–43 (2013). https://doi.org/10.1016/j.cageo.2012.09.008
5. Guibert, R., Nazarova, M., Horgue, P., Hamon, G., Creux, P., Debenest, G.: Computational Permeability Determination from Pore-Scale Imaging: Sample Size, Mesh and Method Sensitivities. Transport in Porous Media **107**(3), 641–656 (2015). https://doi.org/10.1007/s11242-015-0458-0
6. Tembely, M., AlSumaiti, A.M., Jouini, M.S., Rahimov, K.: The effect of heat transfer and polymer concentration on non-Newtonian fluid from pore-scale simulation of rock X-ray micro-CT. Polymers **9**(10), 509 (2017). https://doi.org/10.3390/polym9100509
7. Blunt, M.J., Bijeljic, B., Dong, H., Gharbi, O., Iglauer, S., Mostaghimi, P., Paluszny, A., Pentland, C.: Pore-scale imaging and modelling. Advances in Water Resources **51**, 197–216 (2013). https://doi.org/10.1016/j.advwatres.2012.03.003
8. Lecun, Y., Bengio, Y., Hinton, G.: Deep learning. Nature **521**(7553), 436–444 (2015). https://doi.org/10.1038/nature14539
9. Van Der Linden, J.H., Narsilio, G.A., Tordesillas, A.: Machine learning framework for analysis of transport through complex networks in porous, granular media: A focus on permeability. Physical Review E **94**(2), 1–16 (2016). https://doi.org/10.1103/PhysRevE.94.022904
10. Ling, J., Kurzawski, A., Templeton, J.: Reynolds averaged turbulence modelling using deep neural networks with embedded invariance. Journal of Fluid Mechanics **807**, 155–166 (2018). https://doi.org/10.1017/jfm.2016.615
11. Pollock, J., Stoecker-Sylvia, Z., Veedu, V., Panchal, N., Elshahawi, H.: Machine learning for improved directional drilling. In: Proceedings of the Annual Offshore Technology Conference, Vol. 4, Offshore Technology Conference, pp. 2496–2504 (2018). https://doi.org/10.4043/28633-ms
12. Sudakov, O., Burnaev, E., Koroteev, D.: Driving digital rock towards machine learning: Predicting permeability with gradient boosting and deep neural networks. Computers and Geosciences **127**, 91–98 (2019). https://doi.org/10.1016/j.cageo.2019.02.002
13. Wu, J., Yin, X., Xiao, H.: Seeing permeability from images: fast prediction with convolutional neural networks. Science Bulletin **63**(18), 1215–1222 (2018). https://doi.org/10.1016/j.scib.2018.08.006
14. Araya-Polo, M., Alpak, F.O., Hunter, S., Hofmann, R., Saxena, N.: Deep learning–driven permeability estimation from 2D images. Computational Geosciences **24**, 571–580 (2020). https://doi.org/10.1007/s10596-019-09886-9
15. Araya-Polo, M., Alpak, F.O., Hunter, S., Hofmann, R., Saxena, N.: Deep learning-driven pore-scale simulation for permeability estimation. In: 16th European Conference on the Mathematics of Oil Recovery, ECMOR 2018, Vol. 2018, European Association of Geoscientists and Engineers, EAGE, pp. 1–14 (2018). https://doi.org/10.3997/2214-4609.201802173
16. Alqahtani, N., Armstrong, R.T., Mostaghimi, P.: Deep learning convolutional neural networks to predict porous media properties. In: Society of Petroleum Engineers - SPE Asia Pacific Oil and Gas Conference and Exhibition 2018, APOGCE 2018, Society of Petroleum Engineers (2018). https://doi.org/10.2118/191906-ms
17. Andrew, M.: A quantified study of segmentation techniques on synthetic geological XRM and FIB-SEM images. Computational Geosciences **22**, 1503–1512 (2018). https://doi.org/10.1007/s10596-018-9768-y
18. Miao, X., Gerke, K.M., Sizonenko, T.O.: A new way to parameterize hydraulic conductances of pore elements: A step towards creating pore-networks without pore shape simplifications. Advances in Water Resources **105**, 162–172 (2017). https://doi.org/10.1016/j.advwatres.2017.04.021
19. Rabbani, A., Babaei, M.: Hybrid pore-network and lattice-Boltzmann permeability modelling accelerated by machine learning. Advances in Water Resources **126**, 116–128 (2019). https://doi.org/10.1016/j.advwatres.2019.02.012
20. Alpak, F.O., Gray, F., Saxena, N., Dietderich, J., Hofmann, R., Berg, S.: A distributed parallel multiple-relaxation-time lattice Boltzmann method on general-purpose graphics processing units for the rapid and scalable computation of absolute permeability from high-resolution 3D micro-CT images. Computational Geosciences **22**(3), 815–832 (2018). https://doi.org/10.1007/s10596-018-9727-7
21. Alpak, F.O., Araya-Polo, M.: Rapid computation of permeability from Micro-CT images On GPGPUs. In: 16th European Conference on the Mathematics of Oil Recovery, ECMOR 2018, European Association of Geoscientists and Engineers, EAGE (2018). https://doi.org/10.3997/2214-4609.201802184
22. Alpak, F.O., Zacharoudiou, I., Berg, S., Dietderich, J., Saxena, N.: Direct simulation of pore-scale two-phase visco-capillary flow on

large digital rock images using a phase-field lattice Boltzmann method on general-purpose graphics processing units. Computational Geosciences **23**(5), 849–880 (2019). https://doi.org/10.1007/s10596-019-9818-0

23. Mosser, L., Dubrule, O., Blunt, M.J.: Reconstruction of three-dimensional porous media using generative adversarial neural networks. Phys. Rev. E **96**, 043309 (2017). https://doi.org/10.1103/PhysRevE.96.043309. https://link.aps.org/doi/10.1103/PhysRevE.96.043309
24. Tembely, M., Attarzadeh, R., Dolatabadi, A.: On the numerical modeling of supercooled micro-droplet impact and freezing on superhydrophobic surfaces. International Journal of Heat and Mass Transfer **127**, 193–202 (2018). https://doi.org/10.1016/j.ijheatmasstransfer.2018.06.104